Comparative Study on the Adsorption of $[AuCl_4]^-$ onto Salicylic Acid and Gallic Acid Modified Magnetite Particles

Maya Rahmayanti[1,2,*], Sri Juari Santosa[2], and Sutarno[2]

[1]*Department of Chemistry, State Islamic University of Sunan Kalijaga, Jl. Marsda Adi Sucipto, Yogyakarta 55281, Indonesia*

[2]*Department of Chemistry, Faculty of Mathematics and Natural Sciences, Universitas Gadjah Mada Sekip Utara PO BOX BLS 21 Yogyakarta 55281, Indonesia*

Received February 12, 2016; Accepted May 10, 2016

ABSTRACT

Salicylic acid-modified magnetite (Mag-SA) and gallic acid-modified magnetite (Mag-GA) particles were prepared by co-precipitation procedure. Characterization results showed the interaction that occurs between the surface of magnetite with salicylic acid (Mag-SA) and gallic acid (Mag-GA) was through hydrogen bonding. Adsorption of $[AuCl_4]^-$ onto Mag-SA and Mag-GA surfaces as a function of initial pH, contact time, and initial concentration of the $[AuCl_4]^-$ solution were comparatively investigated. Result showed that the optimum adsorption of $[AuCl_4]^-$ onto Mag-SA or Mag-GA was found at pH 3. The adsorption process were found to allow the pseudo-second order equation, both for Mag-SA and Mag-GA. The parameters in isotherm adsorption equations conformed to the Langmuir and Freundlich isotherms very well for Mag-GA, but for Mag-SA, only conformed to the Langmuir isotherm very well. The result of this study demonstrate that the ability Mag-GA to adsorb $[AuCl_4]^-$ higher than Mag-SA.

Keywords: *salicylic acid-modified magnetite; gallic acid-modified magnetite; adsorption; $[AuCl_4]^-$*

ABSTRAK

Asam salisilat termodifikasi magnetit (Mag-SA) dan asam galat termodifikasi magnetit (Mag-GA) telah dilakukan melalui metode kopresipitasi. Hasil karakterisasi menunjukkan interaksi yang terjadi antara permukaan magnetit dengan Mag-SA dan Mag-GA terjadi melalui ikatan hidrogen. Adsorpsi $[AuCl_4]^-$ pada permukaan Mag-SA dan Mag-GA sebagai fungsi pH, waktu dan konsentrasi $[AuCl_4]^-$ telah dipelajari dan dibandingkan. Hasil menunjukkan bahwa adsorpsi $[AuCl_4]^-$ pada Mag-SA atau Mag-GA terjadi pada pH optimum 3. Proses adsorpsi untuk kedua adsorben ini mengikuti persamaan orde dua-semu. Parameter isotherm adsorpsi $[AuCl_4]^-$ pada Mag-GA menunjukkan nilai yang sangat baik untuk isoterm Langmuir dan Freundlich, namun untuk adsorpsi $[AuCl_4]^-$ pada Mag-SA hanya menunjukkan nilai yang sangat baik untuk isoterm Langmuir. Hasil penelitian ini menunjukkan bahwa kemampuan Mag-GA dalam mengadsorpsi $[AuCl_4]^-$ lebih baik dibandingkan Mag-SA.

Kata Kunci: *asam salisilat termodifikasi magnetit; asam galat termodifikasi magnetit; adsorpsi; $[AuCl_4]^-$*

INTRODUCTION

Gold is considered as the most versatile metal due to its many unique properties and utilization. These days, apart from the traditional uses, gold has found new applications in electronics, chemical and environmental catalyses, medicine and life sciences [1]. Considering the increasing demand for this metal, while the available natural sources continuously decrease it will open wide opportunity to get the gold back from secondary sources. Indeed gold recovery from secondary sources such as electronic waste is more desirable than that for most other metals. This is why many researchers give great attention for the recovery of gold over the years. Methods which have been applied to the recovery of gold from its solutions include, chelating resins [2], ammoniacal thiosulfate leach liquors [3], and ion exchange [4].

Apart from the above mentioned methods, recovery of gold via adsorption-reduction method using macromolecular compounds that containing many phenolic and carboxylic groups have also developed. Santosa et al. [5] pointed out that humin had the ability to remove $[AuCl_4]^-$ from the aqueous solution. The role of COOH functional group in removing $[AuCl_4]^-$ through hydrogen bonding is more significant for the purified humin, while that of OH group in removing $[AuCl_4]^-$ through reduction to Au metal is better for the crude (unpurified) humin. Other researchers showed that Bayberry tannin-immobilized on mesoporous silica (BT-

* Corresponding author. Tel : +62-81222758535
Email address : mrahmayanti08@gmail.com

SiO_2) was highly effective and selective for the adsorptive recovery of Au(III) from diluted aqueous solutions [6]. The adsorption of Au(III) on BT-SiO_2 was a reductive adsorption process, in which Au(III) was reduced to its elemental form while the phenolic group of tannins was oxidized to quinone. Similarly, the use of persimmon peel gel for the recovery of Au(III) from aqueous chloride medium was investigated by Parajuli et al. [7]. The reduction of Au(III) is accompanied by the exchange of ligands between $[AuCl_4]^-$ and polyphenolic groups of substrates and then followed by reduction of Au(III) to Au(0).

Based on the above mentioned, in this study effort to recover gold from chloride solution was performed using salicylic acid and gallic acid. Salicylic acid has a -COOH group and a -OH group where the OH group is in ortho position to the COOH group. Meanwhile, gallic acid has a –COOH group and three –OH groups. Differences in the amount of phenolic groups owned by salicylic acid salicylic acid (SA) and gallic acid (GA) were expected to affect the ability to absorp metal ions.

On the other hand, magnetic separation has been applied recently in various fields. From an environmental point of view, magnetic separation possesses advantages due to easy recovery of the adsorbent without filtration or centrifugation. Several studies have reported magnetic separation using modified magnetite (Fe_3O_4) as an environmental friendly approach to remove heavy metal ions [8-11] and organic pollutants [12].

The aim of the present study was to modify magnetite with salicylic acid (Mag-SA) and gallic acid (Mag-GA) to study the interactions that may occur between the surface of the magnetite and SA as well as GA and to apply the Mag-SA and Mag-GA to reductively adsorp of $[AuCl_4]^-$.

EXPERIMENTAL SECTION

Materials

The SA and GA powders used were a pure chemical, purchased from Merck (Germany). Iron(II) sulfate heptahydrate ($FeSO_4{\cdot}7H_2O$), ferric chloride hexahydrate ($FeCl_3{\cdot}6H_2O$), sodium hydroxide (NaOH), and hydrochloric acid (HCl) were purchased from Merck (Germany). Carbonate-free distilled water was used for preparation of the solution and for rinsing the products.

Instrumentation

Chemical characteristics of the material were examined using Fourier transform infrared spectroscopy model Shimadzu FTIR-820 IPC. Crystallinity of the materials was determined using Shimadzu XRD-6000. Vibrating Sample Magnetometer (VSM) type OXFORD VSM 1.2 H was used to examine the magnetic properties. The morphology of samples was viewed by scanning electron microscopy (SEM) of a JSM-6360 instrument. Atomic Absorption Spectroscopy (AAS, Analytic Jena ContrAA 300, λ = 242.8 nm) was used to measure the concentrations of $[AuCl_4]^-$ in the adsorption media.

Procedure

Synthesis of magnetite, Fe3O4

An aqueous solution of NaOH at pH 13 was prepared by dissolving the subsequent amount of NaOH in de-ionized water. The NaOH solution was heated at 60 °C. A mixture containing equal volumes of Fe^{3+}(0.25 M) and Fe^{2+}(0.125 M) (was injected into the NaOH solution with vigorous stirring. The whole solution was vigorously stirred at the same constant temperature (60 °C) for 1 h. The precipitation was separated from the aqueous solution by external magnetic decantation, washed with distilled water several times and then dried at 50 °C for 3 h.

Modification of magnetite with salicylic acid

Aqueous solutions of Fe^{3+}, Fe^{2+} and SA were separately prepared by dissolving the respective amounts of $FeCl_3{\cdot}6H_2O$ (10 mL, 1.1 M), $FeSO_4{\cdot}7H_2O$ (10 mL, 0.55 M) and SA (100 mL, 0.44 M) in the distilled water. An aqueous solution of NaOH at pH 13 was also prepared by dissolving the corresponding amount of NaOH in the distilled water. A mixture containing equal volumes of Fe^{3+} and Fe^{2+} was injected into the NaOH solution with vigorous stirring at temperature 60 °C. Once the mixture of Fe^{3+} and Fe^{2+} was complete injected, subsequent SA solution was added quickly to the reaction. The mixed solution was stirred at temperature 60 °C for 1 h. The precipitate was separated from the aqueous solution by external magnetic decantation, washed with distilled water several times and then dried at 50 °C for 3 h. The result of the synthesis referred to as Mag-SA.

Modification of magnetite with gallic acid

The procedure of modification, washing and drying was done the same as Mag-SA, but SA solution was replaced by GA solution. Material that was formed from this procedure referred to as Mag-GA.

Characterization of materials

The magnetite (Mag), Mag-SA and Mag-GA were first characterized for their functional groups by a FTIR spectrometer in the transmission mode in spectroscopic grade KBr pellets for all the powders. An X-ray diffraction (XRD) patterns of samples were

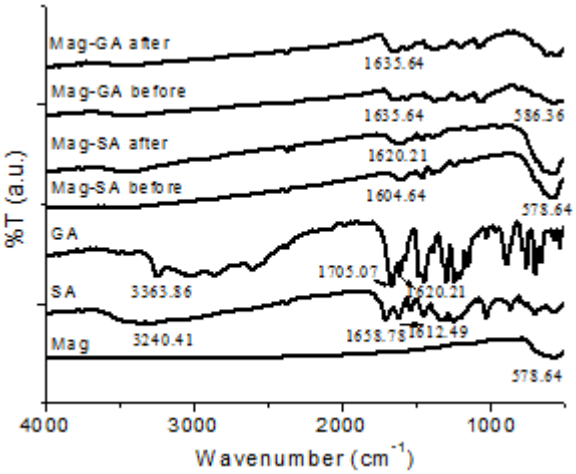

Fig 1. FTIR spectra Mag, SA and GA (before and after modification) and Mag-SA and Mag-GA (before and after adsorption)

recorded using a Shimadzu XRD-6000 diffractometer with Ni-filtered Cu Kα radiation (λ = 0.15406 nm) at voltage 40 kV and current 30 Ma. The samples were scanned in steps of 0.02° (2Θ) in the range from 0 to 70° with a count time of 4 sec per step. VSM (OXPORD VSM 1.2 H) was used for magnetization measurements. These measurements were taken from 0 to 10 kOe field. From these fields versus magnetization curve patterns, saturation magnetization values of the samples were determined. A SEM (JEOL type JED-2300) was used to examine the morphological structure of the samples.

Stability test of Fe in Mag, Mag-SA and Mag-GA

Ten milligrams of Mag was added to a series of 10 mL of distilled water with the acidity that was adjusted to range pH 1-10 using NaOH or HCl solution. Later then the mixture was shaken for 60 min, the supernatant was separated from the solid using external magnet decantation and then the supernatant was analyzed its concentration of Fe using AAS. The same experiments were also conducted for Mag-SA and Mag-GA.

Batch [AuCl4]- adsorption experiments

Adsorption experiments were carried out at room temperature (about 30 °C) using batch process on a shaker.

Effect of medium acidity. A series of $[AuCl_4]^-$ solution (10 mL, 25 ppm) were adjusted to pH 2, 3, 4, 5, 6, and 7 by adding either HCl or NaOH solution. Into every $[AuCl_4]^-$ solution, 10 mg Mag-SA was added, the mixture was shaken at 125 rpm for 60 min, and followed by the phase separation using an external magnet. The residual $[AuCl_4]^-$ solution was determined with AAS. The same experiments were also conducted for Mag-GA.

Adsorption kinetics. Adsorption kinetics was carried out in batch adsorption mode. Into a series $[AuCl_4]^-$ solution (10 mL, 25 ppm) at optimum pH, 10 mg of Mag-SA was added,, shaken at 125 rpm for various contact times and followed by the phase separation using an external magnet. The residual $[AuCl_4]^-$ in every solution was determined with AAS. The same experiments were also conducted for Mag-GA.

Adsorption isotherm. Adsorption isotherm was conducted by using a series of 10 mL $[AuCl_4]^-$ solution with various concentration at optimum pH. Into every $[AuCl_4]^-$ solution, 10 mg Mag-SA added and shaken at 125 rpm for optimum contact time, and followed by the phase separation using an external magnet. The residual $[AuCl_4]^-$ Concentration in the solution was determined with AAS. The same experiments were also conducted for Mag-GA.

RESULT AND DISCUSSION

Characterization of Mag, Mag-SA and Mag-GA

Fig. 1 shows the typical FTIR spectra of Mag, SA, GA, Mag-SA and Mag-GA. The spectra for Mag, Mag-SA and Mag-GA showed the characteristic vibration modes of magnetite particles. The strong and broad absorption band centered at around 578 cm^{-1} corresponds to the Fe-O bonds in the spinel structure of Fe_3O_4. FTIR spectra for GA and SA presents the broad band at around 3400 cm^{-1} which is ascribed to free phenolic O-H stretching and a band at 3240 cm^{-1} is due to acidic O-H stretching. Few bands at 2400-3100 cm^{-1} correspond to C-H stretching mode. The absorption bands at 1700 and 1450 cm^{-1}, were attributed to asymmetric and symmetric vibrations of COOH, respectively. The intense peak at 1620 and 1612 cm^{-1} is due to C=C stretching vibration of the aromatic ring whereas a band around 1350 cm^{-1} is corresponded to –CH- bending vibration of benzene ring. A band at 1026 cm^{-1} is due to the C-O stretching and a band at around 1310 cm^{-1} is attributed to O-H bending vibration of phenolic group of SA and GA [13].

FTIR spectra of Mag-SA showed the presence of a shift in the band at around 1600 cm^{-1}. This was presumably attributed to the -COOH group which has undergone a process of conjugation due to its interaction with the surface of magnetite. Different from Mag-SA, FTIR spectrum of Mag-GA showed that the band at around 1600 cm^{-1} was not shifted, just the intensity decreased.

Based on FTIR spectra of Mag-SA after adsorption, it appears that a shift in absorption occurs also in the band at around 1604 cm^{-1} to 1620 cm^{-1} with increased intensity which supposedly came from the overlapping -C=O carboxylate with the -C=O quinone group, if Au(III) was reduced to Au(0) by phenolic group. The intensity enhancement of the band at around

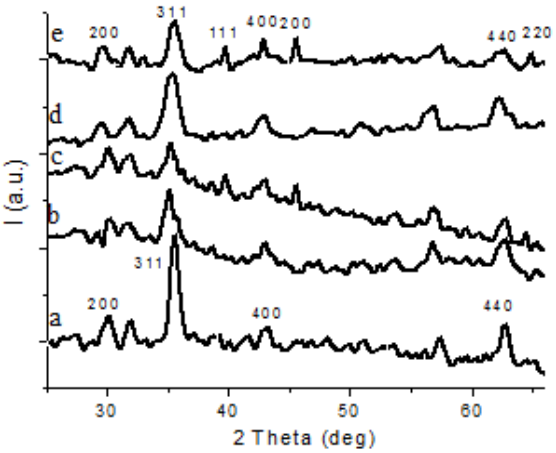

Fig 2. XRD patterns of Mag (a), Mag-SA before (b) and after adsorption (c) and Mag-GA before (d) and after adsorption (e)

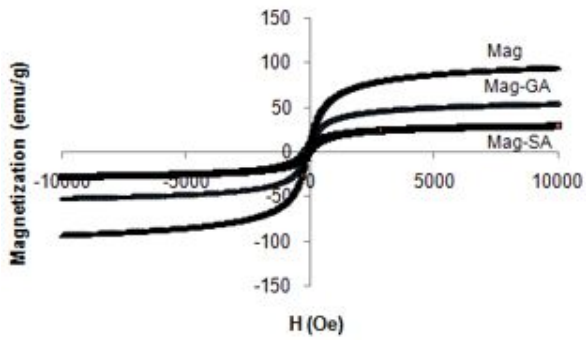

Fig 3. Magnetization curve at room temperature for Mag-SA and Mag-GA

3400 cm^{-1} was derived from the protonation of the -C=O carboxylic group. The appearance of band at around 580 cm^{-1} was characteristic of Fe-O bond, and it confirmed that the magnetite did not play a role in the process of adsorption-reduction, but the presence of magnetite in the adsorbent play a role in the separation of the adsorbent from the adsorbate. In addition, the presence of magnetite in the adsorbent could be expected to improve transport of $[AuCl_4]^-$ from solution to Mag-SA or Mag-GA. The emergence of band at around 620 cm^{-1} probably derived from Au-O bond, so that not all Au(III) attracted by Mag-SA and Mag-GA to be reduced to Au(0). To prove Au(III) actually been partly reduced, further characterization using XRD diffractogram was performed.

The crystalline structure of magnetite before and after modification showed in Fig. 2a, 2b, and 2c. The diffraction peaks of (220), (311), (400), (511), and (440) reflect the magnetite crystal. They correspond to the standard data for Fe_3O_4 (JCPDS no. 89.0691). The XRD patterns showed the peaks of Mag were sharper than those of Mag-SA and the peaks of Mag-GA were sharper than those of Mag-SA which indicated that crystallinity magnetite before modification were higher than after modification with SA and GA. After modification, 2Θ of the characteristic peaks of Mag was not significantly different. Characteristics of gold metal appear at 2θ = 37.97°; 44.16°; 64.44° although with low intensity. These three peaks were equal to the peak pattern of gold diffractogram obtained by Huang et al. [6], Ogata and Nakano [14] and Castro et al. [15]. The characteristic peaks are for the reflection field [111], [200], and [220].

The value of saturation magnetization of Mag decreased after the modification process (Fig. 3). After Mag modified by SA and GA, Ms Mag reduced from 93.90 emu/g to 53.18 emu/g (MAG-SA) and 28.31 emu/g (Mag-GA). This was possible because the Mag has interacted with SA and GA, which were non magnetic compounds that can reduce the magnetic interaction between the particles. Salicylic acid or GA on Mag layer can reduce surface moment of magnetite and ultimately reduce the magnetic moment in the particles.

Fig. 4 shows the SEM images of magnetite before and after modification with SA and GA as well as those of SA and GA. Apparently, the morphology of the Mag-SA and Mag-GA were different. The morphological structure of Mag-SA was more resembles to that of magnetite before modification, but for Mag-GA, its morphological structure showed the presence of GA on the surface of Mag particles. This occurs related to the interaction that formed between the surface of the Mag with SA and GA were described later.

Comparison of Interaction Models that Occurs in the Modification

Modification of Mag with SA was conducted at pH 6, which was smaller than pH_{PZC} magnetite (6 to 6.8) [18] so that the surface of the magnetite tend to be positive due to protonation. On the other hand the -COOH group of SA at this pH has been ionized to $-COO^-$ since the pK_{a1} SA is 3 [19]. Thus the interaction between the surfaces of magnetite with $-COO^-$ group possibly would occur through hydrogen bonding (Fig. 5). Based on the pK_{a2} of SA, -OH group of SA has begun ionized at this pH, so it was possible that the interaction between the surface of the magnetite with $-O^-$ group. These processes cause the intensity of the absorption band at around 3400 cm^{-1} decrease after modification.

Preparation of Mag with GA was occurred at pH of 8-9 where this pH value is higher than the pH_{PZC} Mag. Magnetite surfaces tend to be negative, while the –COOH and –OH groups of GA were ionized, so that the interaction between the surface of the magnetite

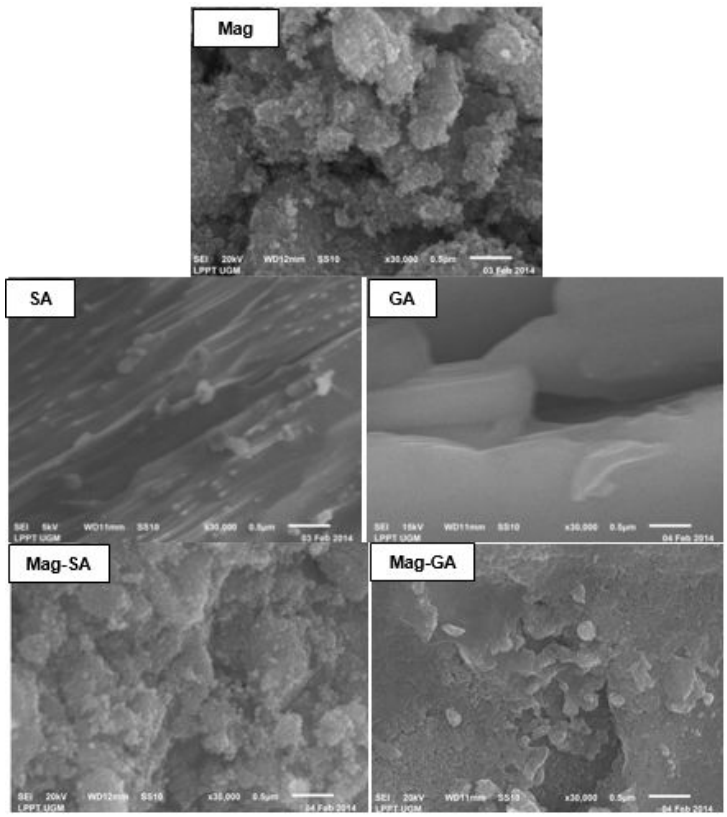

Fig 4. Comparison of SEM images for magnetite, SA, and GA particles, before and after modification

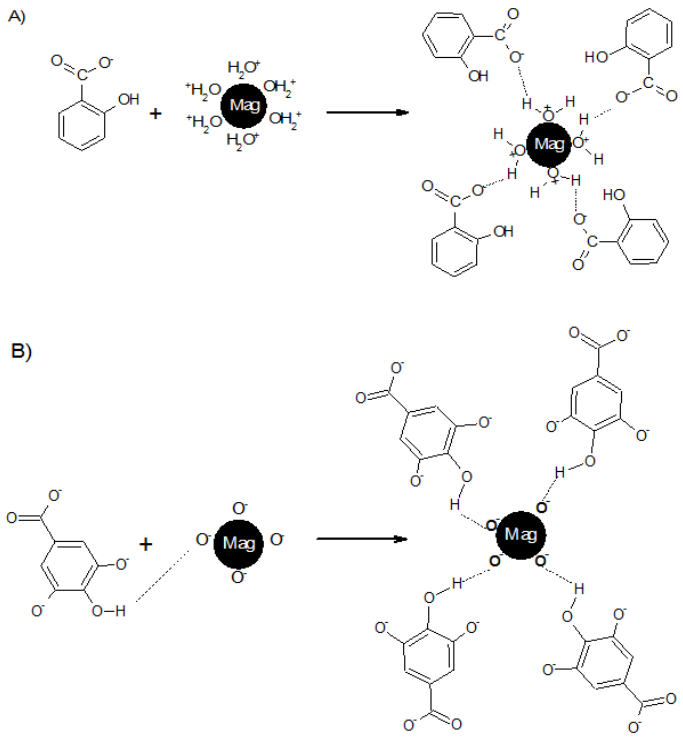

Fig 5. Alleged interaction model salicylic acid (A) and gallic acid (B) on magnetite

and -COO$^-$ and -OH$^-$ is difficult to occur due to electrostatic interaction. This process causes the band at around 3400 cm^{-1} still appears after modification. Suggested interactions that occur between the Mag with GA is through hydrogen bonds between phenolic groups which were not ionized and the surface of magnetite. Alleged model of interaction that occurs between the surface of magnetite with SA and GA were presented in Fig. 5.

Stability of Magnetites in Mag-SA and Mag-GA

The result showed the concentration of Fe in the filtrate of Mag-SA and Mag-GA are smaller than the concentration of Fe in the filtrate of Mag (Fig. 6). Thus, it can be said that the stability of magnetite increased after magnetite modified with SA and GA and the stability of magnetite at Mag-GA was higher than the stability of magnetite at Mag-SA (Fig. 6).

Effect of pH on the adsorption of [AuCl4]$^-$ onto Mag-SA and Mag-GA

The effect of pH on the adsorption of $[AuCl_4]^-$ onto Mag-SA and Mag-GA was shown in Fig. 7, where 10 mg Mag-SA/Mag-GA was utilized to adsorb $[AuCl_4]^-$

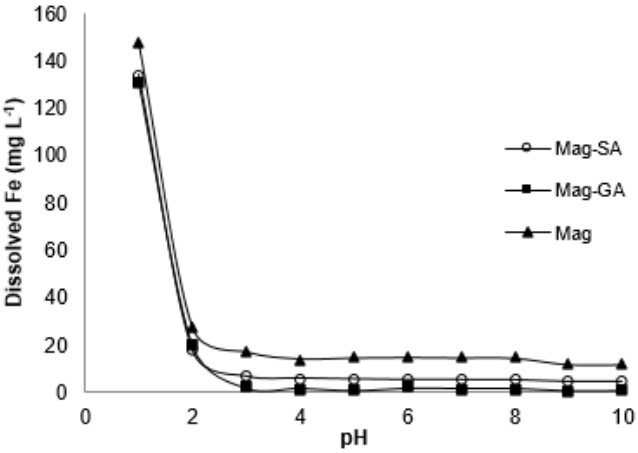

Fig 6. Stability curve magnetites in Mag-SA and Mag-GA

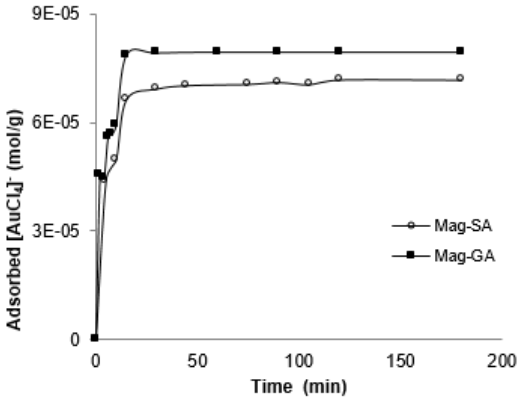

Fig 8. Effect of contact time on the adsorption of $[AuCl_4]^-$ on Mag-SA and Mag-GA (initial $[AuCl_4]^-$ concentration 25 mg/L; solution volume 10 mL; adsorbent dose 0.01 g)

solution (10 mL, 25 mg/L). The pH of solution was adjusted by HCl or NaOH and all pH measurements were carried out using digital pH meter. The result showed the adsorption of $[AuCl_4]^-$ on the surface of the Mag-SA and Mag-GA was significantly influenced by the pH. It was attributed to a change in pH of the solution results in forming different ionic species and different surface charge of Mag-SA and Mag-GA. When the pH of the system was low (2-3), –OH group is unionized, while the charge of $[AuCl_4]^-$ was negative. Therefore, it was possible to form hydrogen bonding between the surface of Mag-SA and Mag-GA and $[AuCl_4]^-$ [20]. The optimum adsorption occurred at pH 3 for Mag-SA and Mag-GA. Above pH 3, the –OH group has begun ionized so the surface of Mag-SA and Mag-GA was more negative. Hence, the interaction between $[AuCl_4]^-$ with the surface of Mag-SA and Mag-GA was getting weaker. Consequently, the amount of $[AuCl_4]^-$ that adsorbed decreases with increasing pH. Distribution complex of ions Au(III) in aqueous solution in various pH also affects the adsorption process $[AuCl_4]^-$ onto the

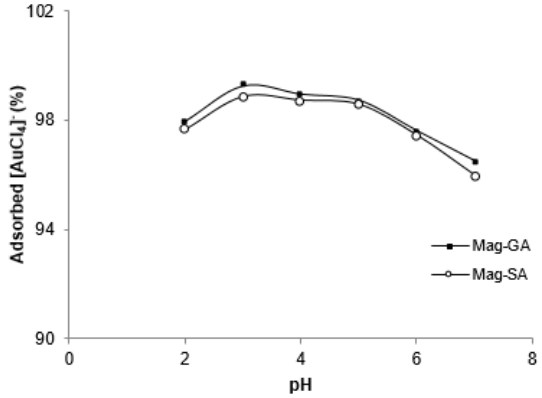

Fig 7. Effect of pH on the adsorption of $[AuCl_4]^-$ onto Mag-SA and Mag-GA (initial $[AuCl_4]^-$ concentration 25 mg/L; solution volume 10 mL; adsorbent dose 0.01 g)

Mag-SA and Mag-GA. Species of $[AuCl_4]^-$ decreases with increasing pH due to an exchange -Cl with -OH so $[AuCl_{4-n}(OH)n]^-$ species is increasing in the solution [21]. Thus, the interaction $[AuCl_4]^-$ with Mag-SA and Mag-GA decreases. Lower adsorbed $[AuCl_4]^-$ at pH 2 was caused by the fact that Mag in Mag-SA and Mag-GA were not stable at this pH and species of $[AuCl_4]^-$ was lower at this pH.

Effect of Contact Time on the Adsorption of $[AuCl4]^-$ onto Mag-SA and Mag-GA

Fig. 8 showed in the early minutes up to 30 min, adsorption of $[AuCl_4]^-$ onto Mag-SA was rapid and then slow down with the increasing contact time. In the early minutes nearly all active sites on the surface of Mag-SA are still empty, this condition makes it easier to interact with $[AuCl_4]^-$ until the adsorption equilibrium was reached at minute 60. After equilibrium was reached, no significant increase or decrease in the adsorbed amount of $AuCl_4^-$ was observed. Different to the Mag-SA, time of equilibrium was more rapid in the adsorption $[AuCl_4]^-$ on Mag-GA, equilibrium reached at minute 30. It maybe influenced by the amount of –OH group owned by GA which is more than SA, thus helping faster adsorption process.

Adsorption Kinetics

Santosa's first order and Ho's pseudo second-order were employed to perform the kinetic study. The linier form of the first order rate [16] expression was given as Eq. 1.

$$\ln\frac{\frac{C_0}{C_A}}{C_A} = \frac{kt}{C_A} + K \qquad (1)$$

where C_0 is the initial concentrations of adsorbate (mol/L), C_A is the remaining concentrations of adsorbate

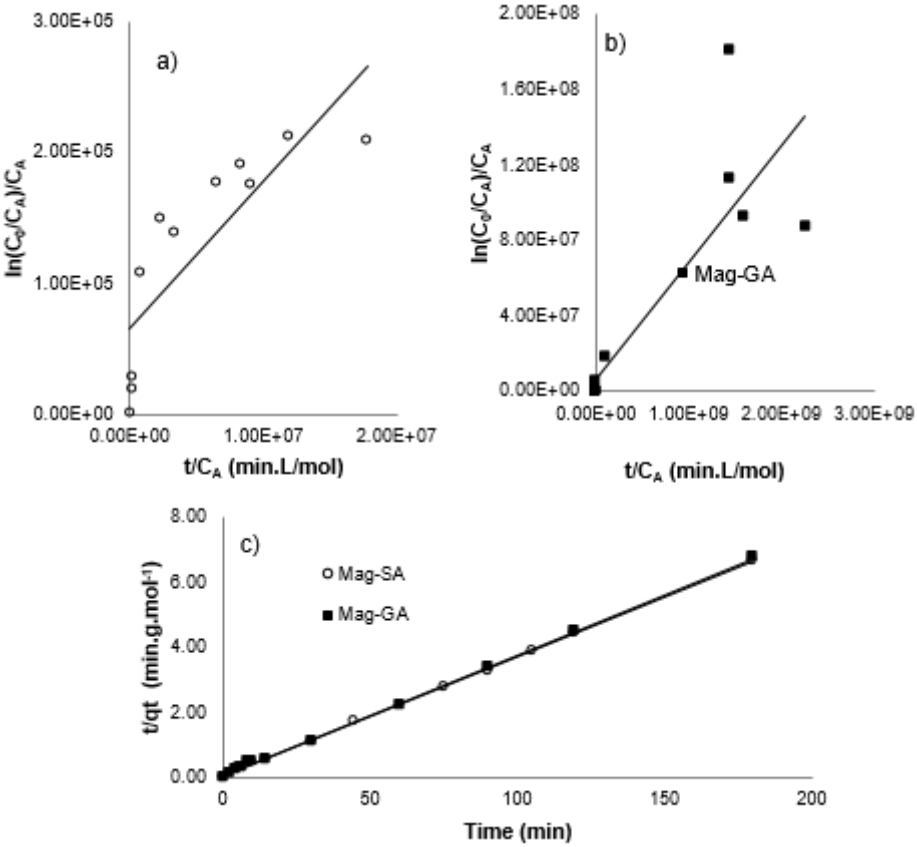

Fig 9. Adsorption kinetics of $[AuCl_4]^-$ on Mag-SA and Mag-GA fitted to the first order equation (a,b), and pseudo-second order equation (c); (adsorbent dose 0.01 g, reaction temperature 30 °C, pH 3.0, $[AuCl_4]^-$ concentration 25 mg/L)

Table 1. Calculated values of parameters in the first order equation and pseudo-second order equation of Mag-SA compared with Mag-GA

Adsorbents	First order equation			Pseudo-second order equation			
	r^2	k (min^{-1})	K (L/mol)	r^2	qe (mg/g)	h (mg/g.min)	k (g/mg.min)
Mag-SA	0.685	0.011	66246	0.999	27.40	12.72	0.001272
Mag-GA	0.718	0.038	26562	0.999	27.03	12.20	0.001220

in solution after adsorption at equilibrium (mol/L), k is the Santosa's first order rate constant, K is the equilibrium adsorption constant and t is the interaction time. The plots of ln $(C_0/C_A)/C_A$ versus t/C_A are shown in Fig. 9a and Fig. 9b.

The pseudo-second order equation was applied to the same sorption data, was represented as Eq. 2 [17], where k is the pseudo-second order sorption rate constant, q_e is the amount of adsorbate adsorbed (mol/g) at equilibrium and q_t is the amount of adsorbate adsorbed (mol/g) at time t. If the plot of t/q_t versus t is linear, then k can be determined from the intercept, while the $1/q_e$ is the slope of the plot. The plots of t/q_t versus t are shown in Fig. 9c.

$$\frac{t}{q_t} = \frac{1}{kq_e^2} + \frac{1}{q_e}t \quad (2)$$

The kinetic parameters acquired from fitting results were summarized in Table 1. For quantitative evaluation of the best kinetic model, correlation coefficients (r^2) were compared. Accordingly as shown in Table 1, the adsorption of $[AuCl_4]^-$ onto Mag-SA and Mag-GA perfectly fits pseudo-second order model rather than first order one.

Adsorption Isotherms

In order to quantitatively explained the adsorption of $[AuCl_4]^-$ onto Mag-SA and Mag-GA, Langmuir and Freundlich adsorption equations were both fitted to the

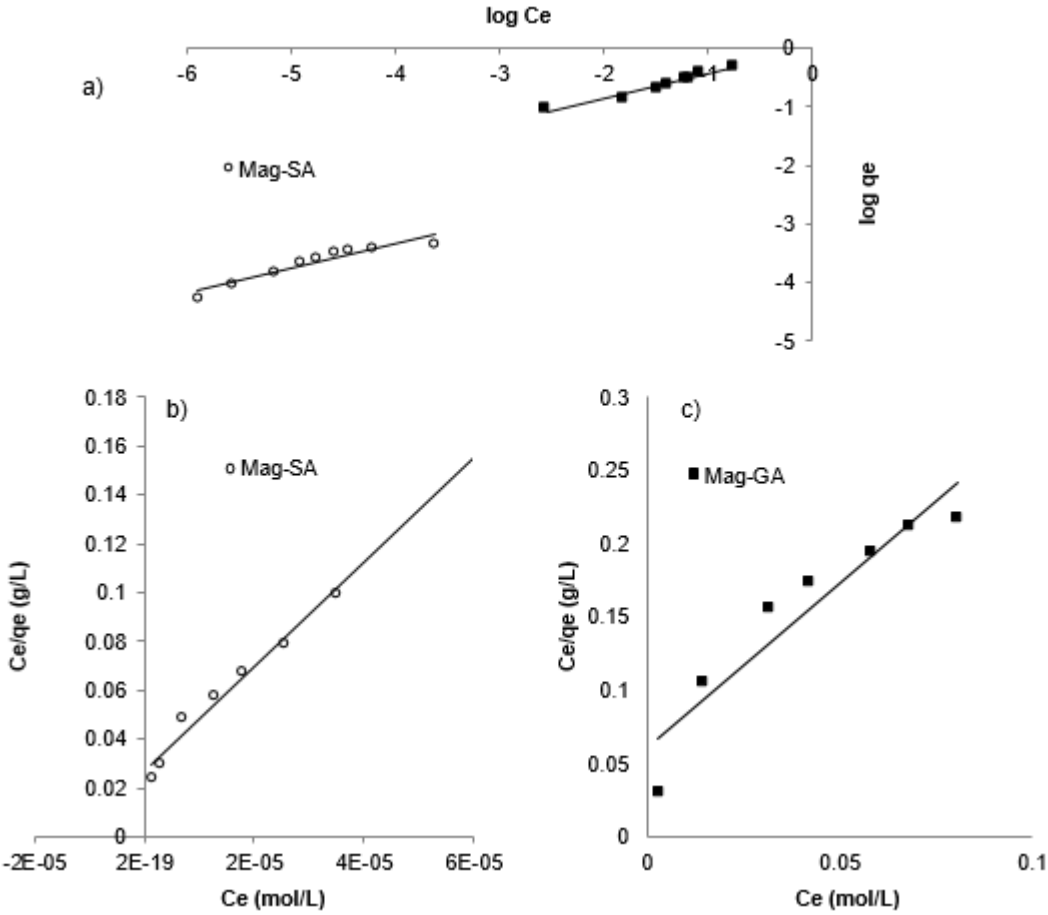

Fig 10. Isotherm adsorption of $[AuCl_4]^-$ on Mag-SA and Mag-GA which is fitted to the Freundlich equation (a), and Langmuir equation (b and c); (adsorbent dose 0.01 g, reaction time 60 min for Mag-SA and 30 min for Mag-GA, reaction temperature 30 °C, pH 3.0)

Table 2. Calculated values of parameters in Langmuir and Freundlich equations

Adsorbents	Langmuir equation				Freundlich equation		
	q_{max} (mol/g)	K_L (L/mol)	E_{ads} (Kj/mol)	r^2	K_F (mol/g)	n	r^2
Mag-SA	0.00047	82423.1	28.516	0.991	0.022	2.37	0.887
Mag-GA	0.00060	17851.06	24.662	0.944	0.019	2.33	0.968

adsorption results. The linear form of Langmuir and Freundlich equations were expressed in Eq. 3 and Eq. 4, respectively.

$$\frac{Ce}{q_e} = \frac{1}{q_{max}K_L} + \frac{C_e}{q_{max}} \quad (3)$$

$$\log q_e = \log K_F + 1/n \log C_e \quad (4)$$

where q_{max} is defined as the capacity of adsorbent (mol/g), q_e is the equilibrium adsorptive quantity of the adsorbate per gram of adsorbent (mol/g), C_e is the equilibrium adsorbate concentration (mol/L). K_L and K_F is the Langmuir and Freundlich adsorption constant respectively, and n is the Freundlich exponential coefficient.

The experimental data and the fitted isotherms of $[AuCl_4]^-$ onto Mag-SA and Mag-GA were represented in Fig. 10. Isotherm parameters for $[AuCl_4]^-$ were calculated from the slope and intercept of the Eq. 3 and Fig. 10 (shown in Table 2). For the adsorption of $[AuCl_4]^-$ onto Mag-SA, gave correlation coefficient for Langmuir equation ($r^2 > 0.991$) which was better than Freundlich equation ($r^2 > 0.888$). It is assumes that the adsorption of $[AuCl_4]^-$ onto Mag-SA occurs in a monolayer, or the adsorption may only occur at a fixed number of localized sites on a surface in which all

adsorption sites are identical and energetically equivalent. In comparison, the adsorption of $[AuCl_4]^-$ onto Mag-GA, the correlation coefficients were satisfactory ($r^2 > 0.90$) for both equations, and the data were better fitted by Freundlich model. It is an indication that surface heterogeneity of the adsorbent can not be neglected. When viewed from the Langmuir equation (Table 2), the capacity (q_{max}) adsorption of $[AuCl_4]^-$ onto Mag-GA larger than that of Mag-SA and the energy of adsorption (E_{ads}) was lower for Mag-GA than Mag-SA. The higher amount of $[AuCl_4]^-$ adsorbed on Mag-GA may be caused by the fact that GA contains more phenolic groups than SA.

CONCLUSION

The interaction that occurred between the surface of Mag and SA and between Mag and GA was governed by hydrogen bond. The hydrogen bonding was between protonated Mag and –COO- for Mag-SA and between Mag and phenolic OH for Mag-GA. The adsorption of $[AuCl_4]^-$ on both Mag-SA and Mag-GA was found to allow the pseudo-second order. The isotherm adsorption equation of $[AuCl_4]^-$ onto Mag-SA was better described by the Langmuir model, while that onto Mag-GA fitted better to the Freundlich model.

REFERENCES

1. Lam, K.F., Fong, C.M., and Yeung, K.L., 2007, *Gold Bull.*, 40 (3), 192–198.
2. Donia, A.M., Atia, A.A., and Elwakeel, K.Z., 2005, *Sep. Purif. Technol.*, 42 (2), 111–116.
3. Grosse, A.C., Dicinoski, G.W., Shaw, M.J., and Haddad, P.R., 2003, *Hydrometallurgy*, 69 (1-3), 1–21.
4. Hubicki, Z., Leszczyńska, M., Łodyg, B., and Łodyga, A., 2006, *Miner. Eng.*, 19 (13), 1341–1347.
5. Santosa, S.J., Sudiono, S., Siswanta, D., Kunarti, E.S., and Dewi, S.R., 2011, *Adsorpt. Sci. Technol.*, 29 (8), 733–746.
6. Huang, X., Wang, Y., Liao, X., and Shi, B., 2010, *J. Hazard. Mater.*, 183 (1-3), 793–798.
7. Parajuli, D., Kawatika H., Inoue, K., Ohto, K., and Kajiyama, K., 2007, *Hydrometallurgy*, 87 (3-4), 133–139.
8. Huang, C., Xie, W., Li, X., and Zhang, J., 2011, *Microchim. Acta*, 173 (1), 165–172.
9. Donia, A.M., Atia, A.A., and Elwakeel, K.Z., 2007, *Hydrometalurgy*, 87 (3-4), 197–206.
10. Shishehbore, M.R., Afkhami, A., and Bagheri, H., 2011, *Chem. Cent. J.*, 5 (1), 41–54.
11. Afkhami, A., and Bagheri, H., 2012, *Microchim. Acta*, 176 (1-2), 217–227.
12. Towler, P.H., Smith, J.D., and Dixon, D.R., 1996, *Anal. Chim. Acta*, 328 (1), 53–59.
13. Rahmayanti, M., Santosa, S.J., and Sutarno, 2015, *Adv. Mater. Res.*, 1101, 286–289.
14. Ogata, T., and Nakano, Y., 2005, *Water Res.*, 39 (18), 4281–4286.
15. Castro, L., Blázquez, M.L., González, F., Muñoz, J.A., and Ballester, A., 2010, *Chem. Eng. J.*, 164 (1), 92–97.
16. Santosa, S.J., Narsito, and Ratna, 2007, *J. Ion Exch.*, 18 (4), 168–173.
17. Ho, Y.S., 2006, *J. Hazard. Mater.*, 136 (3), 681–689.
18. Petrova, T.M., Fachikov, L., and Hristov, J., 2011, *Int. Rev. Chem. Eng.*, 3 (2), 134–152.
19. Friedrich, D.M., Wang, Z., Joly, A.G., Peterson, K.A., and Callis, P.R., 1999, *J. Phys. Chem. A*, 103 (48), 9644–9653.
20. Rahmayanti, M., Santosa, S.J., and Sutarno, 2016, *Int. J. ChemTech Res.*, 9 (4), 446–452.
21. Pacławski, K., and Fitzner, K., 2004, *Metall. Mater. Trans. B*, 35 (6), 1071–1085.